

***Ab initio* calculations of the atomic and electronic structure of CaTiO<sub>3</sub> (001) and (011) surfaces**

R. I. Eglitis and David Vanderbilt

*Department of Physics and Astronomy, Rutgers University, 136 Frelinghuysen Road, Piscataway, New Jersey 08854-8019, USA*

(Received 30 July 2008; revised manuscript received 17 September 2008; published 15 October 2008)

We present the results of calculations of surface relaxations, energetics, and bonding properties for CaTiO<sub>3</sub> (001) and (011) surfaces using a hybrid description of exchange and correlation. We consider both CaO and TiO<sub>2</sub> terminations of the nonpolar (001) surface and Ca, TiO, and O terminations of the polar (011) surface. On the (001) surfaces, we find that all upper-layer atoms relax inward on the CaO-terminated surface, while outward relaxations of all atoms in the second layer are found for both terminations. For the TiO<sub>2</sub>-terminated (001) surface, the largest relaxations are on the second-layer atoms. The surface rumpling is much larger for the CaO terminated than for the TiO<sub>2</sub>-terminated (001) surface, but their surface energies are quite similar at 0.94 and 1.13 eV/cell, respectively. In contrast, different terminations of the (011) CaTiO<sub>3</sub> surface lead to very different surface energies of 1.86, 1.91, and 3.13 eV/cell for the O-terminated, Ca-terminated, and TiO-terminated (011) surface, respectively. Our results for surface energies contrast sharply with those of Zhang *et al.* [Phys. Rev. B **76**, 115426 (2007)], where the authors found a rather different pattern of surface energies. We predict a considerable increase in the Ti-O chemical bond covalency near the (011) surface as compared both to the bulk and to the (001) surface.

DOI: [10.1103/PhysRevB.78.155420](https://doi.org/10.1103/PhysRevB.78.155420)

PACS number(s): 68.35.Ct, 68.35.Md, 68.47.Gh

**I. INTRODUCTION**

Oxide perovskites are in demand for a variety of industrial applications as a result of their diverse physical properties.<sup>1-3</sup> For example, CaTiO<sub>3</sub> is a cubic perovskite that is widely used in electronic ceramic materials and as a key component of synthetic rock to immobilize high-level radioactive waste.<sup>4</sup> Thin films of ABO<sub>3</sub> perovskite ferroelectrics are important for many applications.<sup>1,4</sup> In particular, the titanates are interesting materials regarding their electrochemical properties and are promising as components for electrodes and sensors. Surface properties of CaTiO<sub>3</sub> are important for catalysis and for epitaxial growth of high- $T_c$  superconductors. For all these applications, the surface structure and the associated surface electronic and chemical properties are of primary importance.

In view of this technological importance, it is surprising that there have been so few *ab initio* studies of CaTiO<sub>3</sub> surface atomic and electronic structure. For the CaTiO<sub>3</sub> (001) surface we are only aware of the work of Wang *et al.*<sup>5</sup> and Zhang *et al.*<sup>6</sup> In contrast, several other ABO<sub>3</sub> perovskite (001) surfaces have been widely studied. For example, *ab initio*<sup>7-21</sup> and classical shell-model<sup>22,23</sup> studies were published for the (001) surfaces of SrTiO<sub>3</sub>. The (001) surfaces of cubic perovskites have also been extensively investigated experimentally. For example, the SrTiO<sub>3</sub> (001) surface relaxations and rumplings have been studied by means of low-energy electron-diffraction (LEED), reflection high-energy electron-diffraction (RHEED), medium energy ion scattering (MEIS), and surface x-ray diffraction (SXRD) measurements.<sup>24-28</sup> The status of the degree of agreement between theory and experiment for these SrTiO<sub>3</sub> surfaces is summarized in Ref. 7.

ABO<sub>3</sub> perovskite (011) surfaces are considerably less-well studied than (001) surfaces, both experimentally and theoretically. However, there has been a surge of recent interest focusing mainly on SrTiO<sub>3</sub>, in which STM, UPS, XPS,<sup>29,30</sup>

and Auger spectroscopies, as well as LEED studies,<sup>31-35</sup> have been carried out. On the theory side, the first *ab initio* calculations for SrTiO<sub>3</sub> (011) surfaces were performed by Bottin *et al.*,<sup>36</sup> who carried out a systematic study of the electronic and atomic structures of several (1 × 1) terminations of the (011) polar orientation of the SrTiO<sub>3</sub> surface. They found that the electronic structure of the stoichiometric SrTiO and O<sub>2</sub> terminations showed marked differences with respect to the bulk as a consequence of the polarity compensation. Later, Heifets *et al.*<sup>28</sup> performed *ab initio* Hartree-Fock (HF) calculations for four possible nonpolar terminations (TiO, Sr, and two kinds O terminations) of the SrTiO<sub>3</sub> (011) surface. The authors found that the surface energy of the O-terminated (011) surface is close to that of the (001) surface suggesting that both (011) and (001) surfaces can coexist in polycrystalline SrTiO<sub>3</sub>. Asthagiri and Sholl<sup>37</sup> used density-functional theory (DFT) to determine the energetically preferred structures of submonolayer, monolayer, and multilayer Pt films on both ideal terminations of SrTiO<sub>3</sub> (100), SrTiO<sub>3</sub> (111), and SrTiO<sub>3</sub> (110). The strength of the resulting interfaces between metal and metal-oxide was characterized by the adsorption energy of the film and the film's work of separation. The two polar surfaces SrTiO<sub>3</sub> (111) and SrTiO<sub>3</sub> (110) form significantly stronger interfaces than the nonpolar SrTiO<sub>3</sub> (100) surface. Most recently, we performed an *ab initio* study of SrTiO<sub>3</sub> (011) surfaces<sup>7</sup> using a hybrid HF and DFT exchange-correlation functional, in which HF exchange is mixed with Becke's three-parameter DFT exchange and combined with the nonlocal correlation functional of Perdew and Wang (B3PW).<sup>38,39</sup> Our calculations indicated a remarkably large increase in the Ti-O bond covalency at the TiO-terminated (011) surface significantly larger than for the (001) surfaces.

Regarding other ABO<sub>3</sub> (011) surfaces, Heifets *et al.*<sup>40</sup> investigated the atomic structure and charge redistribution of different terminations of BaZrO<sub>3</sub> (011) surfaces using density-functional methods. They found that the O-terminated (011) surface had the smallest cleavage energy

among (011) surfaces but that this value was still twice as large as the cleavage energy needed for the formation of a pair of complementary (001) surfaces. Moreover, we recently performed *ab initio* B3PW calculations for the technologically important BaTiO<sub>3</sub> and PbTiO<sub>3</sub> (011) surfaces.<sup>41</sup> Our calculated surface energies showed that the TiO<sub>2</sub>-terminated (001) surface is slightly more stable than the BaO- or PbO-terminated (001) surface for both materials and that O-terminated BaTiO<sub>3</sub> and TiO-terminated PbTiO<sub>3</sub> (011) surfaces have surface energies close to that of the (001) surface.

The only existing *ab initio* study of CaTiO<sub>3</sub> (011) polar surfaces was performed by Zhang *et al.*<sup>6</sup> In addition to the (001) surfaces, they studied four possible nonpolar terminations of the (011) surface, namely, the TiO, Ca, asymmetric A-type O, and symmetric B-type O terminations. The results indicated that the most favorable surfaces are the CaO-terminated (001), the A-type O-terminated (011), and the TiO<sub>2</sub>-terminated (001) surfaces, in that order.

With the sole exception of the calculation on CaTiO<sub>3</sub> by Zhang *et al.*,<sup>6</sup> all of the first-principles and shell-model studies of ABO<sub>3</sub> perovskite surface energies<sup>7–12,16,23,28,41,42</sup> have found that the lowest-energy (001) surface is lower in energy than any of the (011) terminations. Zhang *et al.*,<sup>6</sup> on the contrary, reported a surface energy of 0.837 eV per surface cell for their “A-type” O-terminated (011) surface of CaTiO<sub>3</sub> to be compared with 1.021 eV/cell for the TiO<sub>2</sub>-terminated (001) surface. Because this result contrasts sharply with other previous calculations, we were particularly motivated to check this result independently in our current study.

In this study, we have performed predictive *ab initio* calculations for CaTiO<sub>3</sub> (001) and (011) surfaces using the same B3PW approach as in our previous work.<sup>7,41</sup> As in the work of Zhang *et al.*,<sup>6</sup> we do not explicitly include octahedral rotations in the surface calculations even though such rotations are likely to be more important for CaTiO<sub>3</sub> than for many other perovskites; we discuss and justify this approximation at the end of Sec. II. In contradiction to the work of Zhang *et al.*,<sup>6</sup> we find that the pattern of surface energies of CaTiO<sub>3</sub> is similar to that of other perovskites. In particular, we find that the O-terminated CaTiO<sub>3</sub> (011) surface is *higher* in energy than either of the TiO<sub>2</sub>- or CaO-terminated (001) surfaces. We also report the surface relaxations and rumplings and the charge redistributions and changes in bond strength that occur at the surface.

The manuscript is organized as follows. In Sec. II we present our computational method and provide details of the surface slab models on which the calculations were performed. The results of our calculations for surface structures, energies, charge distributions, and bond populations are reported in Sec. III. Finally, we discuss the results and present our conclusions in Sec. IV.

## II. COMPUTATIONAL METHOD AND SURFACE SLAB CONSTRUCTION

To perform the first-principles DFT-B3PW calculations we used the CRYSTAL-2003 computer code,<sup>43</sup> which employs Gaussian-type functions (GTFs) localized at atoms as the basis for an expansion of the crystalline orbitals. The features

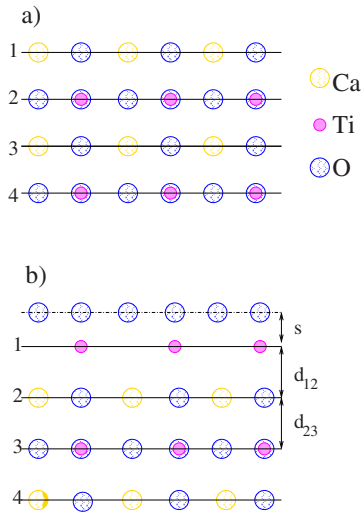
of the CRYSTAL-2003 code that are most important for this study are its ability to calculate the electronic structure of materials within both Hartree-Fock and Kohn-Sham Hamiltonians and its ability to treat isolated two-dimensional (2D) slabs without artificial repetition along the  $z$  axis. However, in order to employ the linear combination of atomic orbitals (LCAO)-GTF method, it is desirable to have optimized basis sets (BS). The BS optimization for SrTiO<sub>3</sub>, BaTiO<sub>3</sub>, and PbTiO<sub>3</sub> perovskites was developed and discussed in Ref. 44. Here we employ this BS, which differs from that used in Refs. 12 and 13, by inclusion of polarizable  $d$  orbitals on O ions. It was shown<sup>44</sup> that this leads to better agreement of the calculated lattice constant and bulk modulus with experimental data. For the Ca atom we used the same BS as in Ref. 45.

Our calculations were performed using the hybrid exchange-correlation B3PW functional involving a hybrid of nonlocal Fock exact exchange, LDA exchange, and Becke’s gradient-corrected exchange functional<sup>38</sup> combined with the nonlocal gradient-corrected correlation potential by Perdew and Wang.<sup>39</sup> The Hay-Wadt small-core effective core pseudopotentials (ECP) were adopted for Ca and Ti atoms.<sup>46</sup> The small-core ECP’s replace only the inner-core orbitals, while orbitals for subvalence electrons as well as for valence electrons are calculated self-consistently. Oxygen atoms were treated with the all-electron BS.

The reciprocal space integration was performed by sampling the Brillouin zone of the five-atom cubic unit cell with an  $8 \times 8 \times 8$  Pack-Monkhorst grid for the bulk<sup>47</sup> and an  $8 \times 8$  grid for the slab structure providing a balanced summation in direct and reciprocal spaces. To achieve high accuracy, large enough tolerances of seven, eight, seven, seven, and 14 were chosen for the Coulomb overlap, Coulomb penetration, exchange overlap, first exchange pseudo-overlap, and second exchange pseudo-overlap parameters, respectively.<sup>43</sup>

The CaTiO<sub>3</sub> (001) surfaces were modeled with two-dimensional slabs consisting of several planes perpendicular to the [001] crystal direction. To simulate CaTiO<sub>3</sub> (001) surfaces, we used slabs consisting of seven alternating TiO<sub>2</sub> and CaO layers with mirror-symmetry preserved relative to the central layer. The 17-atom slab with CaO-terminated surfaces and the 18-atom slab with TiO<sub>2</sub>-terminated surfaces are shown in Figs. 1(a) and 1(b), respectively. These slabs are nonstoichiometric with unit-cell formulae Ca<sub>4</sub>Ti<sub>3</sub>O<sub>10</sub> and Ca<sub>3</sub>Ti<sub>4</sub>O<sub>11</sub>, respectively. These two (CaO and TiO<sub>2</sub>) terminations are the only possible flat and dense (001) surface terminations of the perovskite structure. The sequence of layers with (001) orientation and the definitions of the surface rumpling  $s$  and the interplane distances  $\Delta d_{12}$  and  $\Delta d_{23}$  are illustrated in Fig. 1.

The problem in modeling the CaTiO<sub>3</sub> (011) polar surface is that, unlike the CaTiO<sub>3</sub> (001) neutral surface, it consists of charged O-O and CaTiO planes as illustrated in Fig. 2. Assuming nominal ionic charges of O<sup>2-</sup>, Ti<sup>4+</sup>, and Ca<sup>2+</sup>, a simple cleavage would create a negatively charged O-O surface and a positively charged CaTiO surface leading either to an infinite macroscopic dipole moment perpendicular to the surface for a stoichiometric slab terminated by planes of different kinds (O<sub>2</sub> and CaTiO) as in Fig. 3(a) or to a net infinite charge for a nonstoichiometric symmetric slab as shown in



Figs. 3(b) and 3(c). It is known that such crystal terminations make the surface unstable.<sup>48,49</sup> In proper first-principles calculations on slabs of finite thickness, charge redistributions near the surface arising during the self-consistent field procedure could, in principle, compensate at least partially for these effects. However, previous careful studies for  $\text{SrTiO}_3$  (Refs. 36, 48, and 50) have demonstrated that the resulting surfaces have a high energy and that the introduction of surface vacancies provides an energetically less expensive mechanism for compensating the surfaces.

For these reasons, we limit ourselves here to nonpolar  $\text{CaTiO}_3$  (011) surfaces that have been constructed by modifying the composition of the surface layer. Removing the Ca atom from the upper and lower layers of the 7-layer symmetric  $\text{CaTiO}$ -terminated slab generates a neutral and symmetric 16-atom supercell with  $\text{TiO}$ -terminated surfaces as illustrated in Fig. 3(d). Removing both the Ti and O atoms from the upper and lower layers of the 7-layer symmetric  $\text{CaTiO}$ -terminated slab yields a neutral and symmetric 14-atom supercell with Ca-terminated surfaces as shown in Fig. 3(e). Finally, removing the O atom from the upper and lower lay-

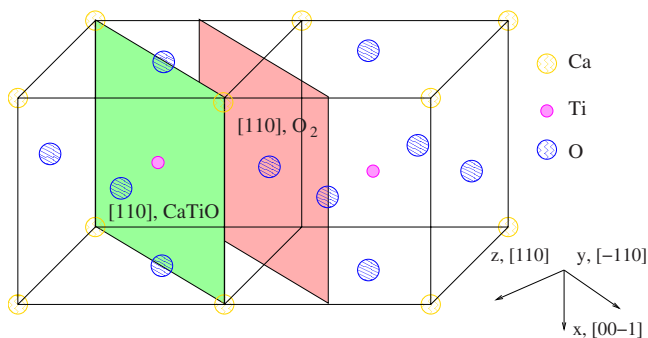


FIG. 2. (Color online) Sketch of the cubic  $\text{CaTiO}_3$  perovskite structure showing two (011) cleavage planes that give rise to charged  $\text{CaTiO}$  and  $\text{O}_2$  (011) surfaces.

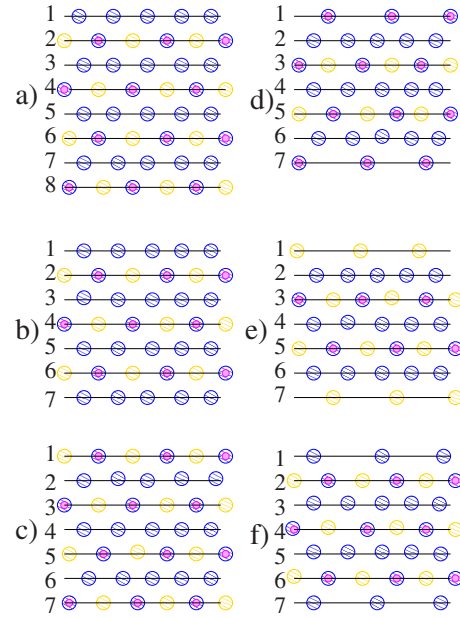


FIG. 3. (Color online) Possible (011) surface slab models considered in the text. [(a)–(c)] Slabs obtained by simple cleavage yielding mixed O-terminated and  $\text{CaTiO}$ -terminated polar surfaces, respectively. [(d)–(f)] Slabs with nonpolar  $\text{TiO}$ -terminated, Ca-terminated, and O-terminated surfaces, respectively.

ers of the 7-layer symmetric O-O terminated slab, we obtain the neutral and symmetric 15-atom supercell with O-terminated surfaces shown in Fig. 3(f). The stoichiometry of these surface terminations and the number of bonds cleaved are comprehensively discussed for the case of  $\text{SrTiO}_3$  in Ref. 36.

Before leaving this section, it is worth discussing the issue of the tilting of  $\text{TiO}_6$  octahedra in  $\text{CaTiO}_3$ . X-ray and neutron-diffraction studies have not definitively established the phase-transition sequence at higher temperature but clearly show that the crystal adopts an orthorhombic structure with space group  $P_{bnm}$  below  $\sim 1380$  K.<sup>51–54</sup> This room-temperature ground state has a 20-atom unit cell and is a slight modification from the ideal perovskite structure involving a pattern of tilts of the  $\text{TiO}_6$  octahedra according to the  $a^-a^+c^+$  pattern in Glazer’s notation.<sup>55</sup> The octahedral tilts have also been studied using first-principles calculations.<sup>56,57</sup> Because these tilts are substantial ( $\sim 10^\circ$ ),<sup>54</sup> it is possible that they may have some impact on the surface structure and energetics. However, we have not included octahedral tilts in the work presented here for several reasons. First, we want to compare with previous calculations, which have universally not included octahedral tilts. Second, the CRYSTAL-2003 code package does not provide for efficient structural optimization as would be needed to study these tilts and the larger surface unit cells that would be required would make the calculations impractical. But finally and most importantly, we estimate that the energy scale of the tilts is only about  $\sim 0.2$  eV per formula unit. This was obtained assuming a simple quadratic-plus-quartic form for the double-well potential in tilt angle  $\theta$  so that  $\Delta E \approx m_O a^2 |\omega^2| \theta^2 / 8$  where  $m_O = 16$  amu is the oxygen mass,  $a = 3.6$  Å is the cubic lattice constant,  $\omega = 219i$  is the zone-center  $R_{25}$  tilt-mode frequency in the par-



TABLE I. Calculated effective charges  $Q$  and bond populations  $P$  (in  $e$ ) for bulk  $\text{CaTiO}_3$ .

Ion or bond	Property	Value
Ca	$Q$	1.782
O	$Q$	-1.371
Ti	$Q$	2.330
Ca-O	$P$	0.006
Ti-O	$P$	0.084
O-O	$P$	-0.010

ent cubic phase,<sup>57</sup> and  $\theta=0.2$  rad is the equilibrium tilt angle.<sup>56,57</sup> This value of  $\sim 0.2$  eV is not negligible but it is still small compared to the energy scale of the surface cleavage and relaxation energies (a few eV), so that it is reasonable to neglect them in a first study. The interaction between bulk tilts and surface relaxations remains an interesting question for future study.

### III. RESULTS OF CALCULATIONS

#### A. $\text{CaTiO}_3$ bulk atomic and electronic structure

As a starting point of our calculations, we calculated the  $\text{CaTiO}_3$  bulk lattice constant and found it to be 3.851 Å, which is slightly smaller than the experimental value of 3.895 Å.<sup>54,58</sup> We used the theoretical bulk lattice constant in the following surface structure calculations. To characterize the chemical bonding and covalency effects, we used a standard Mulliken population analysis for the effective atomic charges  $Q$ , bond populations  $P$ , and other local properties of the electronic structure as described in, e.g., Refs. 59 and 60. Our calculated effective charges and bond populations for bulk  $\text{CaTiO}_3$  are presented in Table I. The bond population of the Ti-O bond is clearly much larger than that of the Ca-O bond consistent with partial Ti-O covalency, and the small but negative O-O population indicates a repulsive overlap of oxygen shells in bulk  $\text{CaTiO}_3$ .

#### B. $\text{CaTiO}_3$ (001) surface structure

The atomic displacements obtained using the *ab initio* B3PW method for  $\text{TiO}_2$ - and CaO-terminated  $\text{CaTiO}_3$  (001) surfaces are shown in Table II. According to the results of

TABLE II. Computed atomic relaxation (in percent of the bulk lattice constant  $a_0$ ) for the  $\text{TiO}_2$ - and CaO-terminated  $\text{CaTiO}_3$  (001) surfaces. Positive values indicate outward displacements.

Layer	CaO terminated		$\text{TiO}_2$ terminated	
	Ion	This study	Ion	This study
1	Ca	-8.31	Ti	-1.71
	O	-0.42	O	-0.10
2	Ti	1.12	Ca	2.75
	O	0.01	O	1.05

TABLE III. Calculated surface rumpling  $s$ , and relative displacements  $\Delta d_{ij}$  between the three near-surface planes, for the CaO- and  $\text{TiO}_2$ -terminated  $\text{CaTiO}_3$  (001) surface. Units are percent of the bulk lattice constant.

$s$	CaO terminated		$\text{TiO}_2$ terminated		
	$\Delta d_{12}$	$\Delta d_{23}$	$s$	$\Delta d_{12}$	$\Delta d_{23}$
7.89	-9.43	1.12	1.61	-4.46	2.75

our calculations, atoms of the first surface layer relax inward, i.e., toward the bulk, for both  $\text{TiO}_2$ - and CaO-terminated (001) surfaces. The latter result is in disagreement with the previous calculations of Wang *et al.*,<sup>5</sup> who calculated that the first-layer oxygen atoms on the (001) surface should relax outward by 0.7% of the bulk lattice constant  $a_0$ . According to our calculations, they move inward by 0.42% of  $a_0$ . Our calculated inward relaxation of the first-layer oxygen atoms on the CaO-terminated  $\text{CaTiO}_3$  (001) surface is in line with previous *ab initio* studies dealing with  $\text{BaTiO}_3$ ,  $\text{PbTiO}_3$ , and  $\text{BaZrO}_3$  (001) surfaces<sup>41,42,61,62</sup> but contrasts with the outward relaxation of first-layer oxygen atoms on the SrO-terminated  $\text{SrTiO}_3$  (001) surface.<sup>7,20,21</sup> According to the results of our current calculations, outward relaxations are found for all atoms in the second layer for both CaO and  $\text{TiO}_2$  terminations of the  $\text{CaTiO}_3$  (001) surface.

Table II shows that the relaxations of the surface metal atoms, which are much larger than those of the oxygens on both the  $\text{TiO}_2$ - and CaO-terminated  $\text{CaTiO}_3$  (001) surfaces, leading to a considerable rumpling of the outermost surface plane. For the  $\text{TiO}_2$ -terminated case, we found much larger displacements in the second layer than in the first layer. This behavior contrasts with the atomic relaxation pattern of the  $\text{TiO}_2$ -terminated  $\text{BaTiO}_3$  (001) surface, where the upper-layer Ti relaxation is generally larger than the second-layer Ba relaxation.<sup>41,61</sup> However, it is in line with the only existing *ab initio* study of the  $\text{TiO}_2$ -terminated  $\text{CaTiO}_3$  (001) surface,<sup>5</sup> as well as with other *ab initio* studies dealing with related  $\text{BO}_2$ -terminated  $\text{ABO}_3$  (001) surfaces, such as  $\text{PbTiO}_3$  (Refs. 41 and 62) and  $\text{BaZrO}_3$ ,<sup>42</sup> where the second-layer anion (Pb or Ba) relaxations were larger than the upper-layer (Ti or Zr) ones.

In order to compare the calculated surface structures with experimental results, the surface rumpling  $s$  (the relative oxygen displacement relative to the metal atom in the surface layer) and the changes in interlayer distances  $\Delta d_{12}$  and  $\Delta d_{23}$  (where 1, 2 and 3 label the near-surface layers) are presented in Table III. Our calculations of the interlayer distances are based on the positions of the relaxed metal ions (Fig. 1), which are known to be much stronger electron scatters than the oxygen ions.<sup>24</sup> The amplitude of the surface rumpling on the CaO-terminated surface is predicted to be almost five times larger than that for the  $\text{TiO}_2$ -terminated (001) one. From Table III, one can see that both  $\text{CaTiO}_3$  (001) surfaces show a reduction in interlayer distance  $\Delta d_{12}$  and an expansion in  $\Delta d_{23}$ . The reduction in interlayer distance  $\Delta d_{12}$  is twice as large for the CaO-terminated surface than it is for the  $\text{TiO}_2$ -terminated surface. Our calculations dealing with the surface rumpling  $s$ , reduction in interlayer distances

TABLE IV. Calculated absolute magnitudes of atomic displacements  $D$  (in Å), effective atomic charges  $Q$  (in  $e$ ), and bond populations  $P$  (in  $e$ ) between nearest metal-oxygen pairs, for the TiO<sub>2</sub>- and CaO-terminated CaTiO<sub>3</sub> (001) surfaces.

Layer	Property	Ion	TiO <sub>2</sub> terminated	Ion	CaO terminated
1	$D$	Ti	-0.066	Ca	-0.320
	$Q$		2.278		1.753
	$P$		0.114		0.020
	$D$	O	-0.004	O	-0.016
	$Q$		-1.267		-1.439
	$P$		0.016		0.070
2	$D$	Ca	0.106	Ti	0.043
	$Q$		1.754		2.335
	$P$		0.006		0.068
	$D$	O	0.041	O	0.000
	$Q$		-1.324		-1.425
	$P$		0.086		0.002
3	$D$	Ti		Ca	
	$Q$		2.326		1.786
	$P$		0.090		0.008
	$D$	O		O	
	$Q$		-1.354		-1.381
	$P$		0.008		0.080

$\Delta d_{12}$ , and expansion in interlayer distances  $\Delta d_{23}$  are in qualitative agreement with the only existing *ab initio* study dealing with CaTiO<sub>3</sub> (001) surface structures.<sup>5</sup>

To the best of our knowledge there are no experimental measurements with which we can compare our calculated values of  $s$ ,  $\Delta d_{12}$ , and  $\Delta d_{23}$  on the CaTiO<sub>3</sub> (001) surfaces. Even when such data do exist, it is sometimes contradictory, as is the case for the SrO-terminated SrTiO<sub>3</sub> (001) surface, where existing LEED (Ref. 24) and RHEED (Ref. 25) experiments contradict each other regarding the sign of  $\Delta d_{12}$ .

The calculated atomic displacements, effective static charges, and bond populations between nearest metal and oxygen atoms are given for the TiO<sub>2</sub>- and CaO-terminated (001) surfaces in Table IV. The major effect observed here is a strengthening of the Ti-O chemical bond near the surface. Recall from Table I that the Ti and O effective charges (2.330 $e$  and -1.371 $e$ , respectively) in bulk CaTiO<sub>3</sub> are much smaller than expected in an ideal ionic model and that the Ti-O bond population is 0.084 $e$ . Table IV shows that the Ti-O bond population for the TiO<sub>2</sub>-terminated (001) surface is considerably larger than the associated bulk value. Comparing with the very small bulk Ca-O bond populations of 0.006 $e$  from Table I, we see that the Ca-O bond populations near the CaO-terminated (001) surface in Table IV are more than three times larger than in the bulk but more than five times smaller than the Ti-O bond populations on the TiO<sub>2</sub>-terminated (001) surface.

### C. CaTiO<sub>3</sub> (011) surface structures

As explained in Sec. II, nonpolar TiO-, Ca-, and O-terminated surfaces can be constructed for the CaTiO<sub>3</sub>

TABLE V. Calculated atomic relaxations of the CaTiO<sub>3</sub> (011) surfaces (in percent of the bulk lattice constant  $a_0$ ) for the three surface terminations. Positive signs correspond to outward displacements.

Layer	Ion	$\Delta z$	$\Delta y$
TiO-terminated surface			
1	Ti	-7.14	
1	O	4.67	
2	O	-0.44	
3	Ca	-2.75	
3	O	-3.79	
3	Ti	-0.78	
Ca-terminated surface			
1	Ca	-16.05	
2	O	1.35	
3	Ti	-0.37	
3	O	-1.71	
3	Ca	-0.93	
O-terminated surface			
1	O	-6.10	-2.16
2	Ti	-0.26	-4.70
2	Ca	-2.10	-0.27
2	O	3.43	8.05
3	O	-0.55	1.90

(011) surface as in Figs. 3(d)–3(f), respectively. Details of the relaxed structures obtained from our calculations for these three terminations are given in Tables V and VI.

On the TiO-terminated (011) surface, the upper-layer Ti atoms move inward by 7.14% of the bulk lattice constant  $a_0$ ; whereas the O atoms move outward by 4.67% (Table V), leading to a large surface rumpling of 11.81% (Table VI), in excellent agreement with the corresponding surface rumpling of 12.10% calculated earlier by Zhang *et al.*<sup>6</sup> The second-layer oxygen atoms move inward by less than 1% of  $a_0$ . The displacement magnitudes of the atoms in the third layer are larger than in the second layer but smaller than in the top layer. The  $\Delta d_{12}$  values in Table VI show that the reduction in the distance between the first and second layers is three times larger than the corresponding expansion between the second and third layers.

On the Ca-terminated (011) surface, Table V shows that the Ca atoms in the top layer move inward very strongly,

TABLE VI. Surface rumpling  $s$  and relative displacements  $\Delta d_{ij}$  (in percent of the bulk lattice constant  $a_0$ ) for the three near-surface planes on the TiO- and O-terminated CaTiO<sub>3</sub> (011) surfaces.

	TiO terminated		O terminated	
	$s$	$\Delta d_{12}$	$\Delta d_{12}$	$\Delta d_{23}$
	11.81	-6.70	-5.84	0.29

while the O atoms in the second layer only move outward very weakly. The pattern of oxygen displacements is similar to that found on the TiO-terminated (011) surface, in that the inward oxygen displacement in the third layer is larger than the outward displacement in the second layer; but the Ti and Ca displacements in the third layer are smaller than the second-layer oxygen atom displacements.

The O-terminated (011) surface has sufficiently low symmetry that some displacements occur in the  $y$  as well as in the  $z$  direction. The O atoms in the top layer move mostly inward ( $\sim 6\%$ ) but also have some displacement along the surface ( $\sim 2\%$ ). On the other hand, the second-layer Ti atoms on this surface move strongly along the surface and also slightly inward. The second-layer Ca atoms move slightly in the same  $y$  direction and also inward, while the second-layer O atoms move very strongly in the  $y$  direction (but in the opposite direction compared to the top-layer O atoms) and rather strongly outward. The third-layer O atoms move in the same direction as the second-layer O atoms along the  $y$  axis; but their displacement magnitude are more than four times smaller and they also move slightly inward. Table VI shows that there is a substantial contraction of the interlayer distance  $\Delta d_{12}$  and only a very slight expansion of  $\Delta d_{23}$ .

#### D. CaTiO<sub>3</sub> (001) and (011) surface energies

In the present work, we define the unrelaxed surface energy of a given surface termination  $\Lambda$  to be one half of the energy needed to cleave the crystal rigidly into an unrelaxed surface  $\Lambda$  and an unrelaxed surface with the complementary termination  $\Lambda'$ . For CaTiO<sub>3</sub>, for example, the unrelaxed surface energies of the complementary CaO- and TiO<sub>2</sub>-terminated (001) surfaces are equal, as are those of the TiO- and Ca-terminated (011) surfaces. The relaxed surface energy is defined to be the energy of the unrelaxed surface plus the (negative) surface relaxation energy. These definitions are chosen for consistency with Refs. 12 and 28. Unlike the authors of Refs. 36, 40, and 63, we have made no effort to introduce chemical potentials here. Thus, while the values of the surface energies  $E_{\text{surf}}$  reflect the cleavage energies and thus give some information about trends in the surface energetics, they should be used with caution when addressing questions of the relative stability of surfaces with different stoichiometries in specific environmental conditions.

To calculate the CaTiO<sub>3</sub> (001) surface energies, we start with the cleavage energy for the unrelaxed CaO- and TiO<sub>2</sub>-terminated surfaces. In our calculations the two 7-layer CaO- and TiO<sub>2</sub>-terminated slabs containing 17 and 18 atoms, respectively, represent together seven bulk unit cells of five atoms each. Surfaces with both terminations arise simultaneously under cleavage. According to our definition, we assume that the relevant cleavage energy is distributed equally between created surfaces so that both the CaO- and TiO<sub>2</sub>-terminated surfaces end up with the same unrelaxed surface energy

$$E_{\text{surf}}^{(\text{unr})} = \frac{1}{4} [E_{\text{slab}}^{(\text{unr})}(\text{CaO}) + E_{\text{slab}}^{(\text{unr})}(\text{TiO}_2) - 7E_{\text{bulk}}], \quad (1)$$

where  $E_{\text{slab}}^{(\text{unr})}(\text{CaO})$  and  $E_{\text{slab}}^{(\text{unr})}(\text{TiO}_2)$  are the unrelaxed CaO- and TiO<sub>2</sub>-terminated slab energies,  $E_{\text{bulk}}$  is the energy per

TABLE VII. Calculated cleavage, relaxation, and surface energies for CaTiO<sub>3</sub> (001) and (011) surfaces (in electron volt per surface cell).

Surface	Termination	$E_{\text{surf}}^{(\text{unr})}$	$E_{\text{rel}}$	$E_{\text{surf}}$
CaTiO <sub>3</sub> (001)	TiO <sub>2</sub>	1.40	-0.27	1.13
	CaO	1.40	-0.46	0.94
CaTiO <sub>3</sub> (011)	TiO	4.61	-1.48	3.13
	Ca	4.61	-2.70	1.91
	O	3.30	-1.44	1.86

bulk unit cell, and the factor of 1/4 comes from the fact that we create four surfaces upon the cleavage procedure. Our calculated unrelaxed surface energy for these surfaces is 1.40 eV/cell as shown in Table VII. The corresponding relaxation energies are calculated using

$$E_{(\text{rel})}(\Lambda) = \frac{1}{2} [E_{\text{slab}}^{(\text{rel})}(\Lambda) - E_{\text{slab}}^{(\text{unr})}(\Lambda)], \quad (2)$$

where  $\Lambda = \text{CaO}$  or  $\text{TiO}_2$  and  $E_{\text{slab}}^{(\text{rel})}(\Lambda)$  is the slab energy after both sides of the slab have been allowed to relax. We find relaxation energies of -0.27 and -0.46 eV for the TiO<sub>2</sub>-terminated and CaO-terminated surfaces, respectively. The final surface energies are then obtained as a sum of the cleavage and relaxation energies using

$$E_{\text{surf}}(\Lambda) = E_{\text{surf}}^{(\text{unr})}(\Lambda) + E_{(\text{rel})}(\Lambda). \quad (3)$$

The resulting surface energies of the two (001) surfaces are comparable but that of the TiO<sub>2</sub>-terminated surface is slightly larger than that of the CaO-terminated one (1.13 vs 0.94 eV/cell), as summarized in Table VII.

In order to calculate the surface energies of the TiO- and Ca-terminated surfaces shown in Figs. 3(d) and 3(e) containing 16 and 14 atoms, respectively, we start with the cleavage energy for unrelaxed surfaces. The two 7-plane Ca- and TiO-terminated slabs represent together six bulk unit cells. The surfaces with both terminations arise simultaneously under cleavage of the crystal, and the relevant cleavage energy is divided equally between these two surfaces; so we obtain cleavage energies according to

$$E_{\text{surf}}^{(\text{unr})}(\Lambda) = \frac{1}{4} [E_{\text{slab}}^{(\text{unr})}(\text{Ca}) + E_{\text{slab}}^{(\text{unr})}(\text{TiO}) - 6E_{\text{bulk}}], \quad (4)$$

where  $\Lambda$  denotes Ca or TiO,  $E_{\text{slab}}^{(\text{unr})}(\Lambda)$  is the energy of the unrelaxed Ca or TiO terminated (011) slab,  $E_{\text{bulk}}$  is the energy per bulk unit cell, and again the factor of 1/4 arises because four surfaces are created upon cleavage. Our calculated cleavage energy for the Ca or TiO-terminated (011) surfaces of 4.61 eV is more than three times larger than the relevant cleavage energy for the CaO- or TiO<sub>2</sub>-terminated (001) surfaces. Finally, the surface energy  $E_{\text{surf}}(\Lambda)$  is just a sum of the cleavage and relaxation energies as in Eq. (3).

When we cleave the crystal along (011) in another way, as in Fig. 3(f), we obtain two identical O-terminated surface slabs containing 15 atoms. The cleavage energy of 3.30 eV computed for this O-terminated surface is slightly smaller

TABLE VIII. Calculated Mulliken atomic charges  $Q$  and their changes  $\Delta Q$  with respect to the bulk in  $e$  for the three  $\text{CaTiO}_3$  (011) surface terminations. For reference, the bulk values are  $2.330e$  (Ti),  $-1.371e$  (O), and  $1.782e$  (Ca).

Atom (layer)	$Q$	$\Delta Q$
TiO-terminated surface		
Ti(I)	2.204	-0.126
O(I)	-1.290	0.081
O(II)	-1.139	0.232
Ca(III)	1.733	-0.049
Ti(III)	2.309	-0.021
O(III)	-1.302	0.069
O(IV)	-1.375	-0.004
Ca-terminated surface		
Ca(I)	1.676	-0.106
O(II)	-1.488	-0.117
Ca(III)	1.781	-0.001
Ti(III)	2.334	0.004
O(III)	-1.452	-0.081
O(IV)	-1.363	0.008
O-terminated surface		
O(I)	-1.139	0.232
Ca(II)	1.751	-0.031
Ti(II)	2.235	-0.095
O(II)	-1.422	-0.051
O(III)	-1.359	0.012
Ca(IV)	1.774	-0.008
Ti(IV)	2.310	-0.020
O(IV)	-1.398	-0.027

than for the Ca or TiO-terminated (011) surfaces, but still more than twice as large as for the (001) surfaces. The unit cell of the 7-plane O-terminated slab has the same contents as three bulk unit cells, so the relevant surface energy is just

$$E_{\text{surf}}(\text{O}) = \frac{1}{2}[E_{\text{slab}}^{(\text{rel})}(\text{O}) - 3E_{\text{bulk}}], \quad (5)$$

where  $E_{\text{surf}}(\text{O})$  and  $E_{\text{slab}}^{(\text{rel})}(\text{O})$  are the surface and the relaxed slab total energies for the O-terminated (011) surface. The results are again summarized in Table VII. Unlike for the (001) surface, we see that different terminations of the (011) surface lead to large differences in the surface energies. Here the lowest calculated surface energy is 1.86 eV/cell for the O-terminated (011) surface, while the TiO-terminated (3.13 eV/cell) is much more costly than the Ca-terminated (011) surface (1.91 eV/cell).

#### E. $\text{CaTiO}_3$ (011) surface charge distributions and chemical bondings

We present in Table VIII the calculated Mulliken effective

charges  $Q$  and their changes  $\Delta Q$  with respect to the bulk values for atoms near the surface for the various (011) surface terminations.

On the TiO-terminated surface, the charge on the surface Ti atom is seen to be substantially reduced relative to the bulk, while the metal atoms in the third layer lose much less charge. The O ions in all layers, except the central one, also have reduced charges making them less negative. The largest charge change ( $0.232e$ ) is observed for subsurface O atoms giving a large positive change of  $0.464e$  in the charge for that subsurface layer.

On the Ca-terminated surface, negative changes in the charges are observed for all atoms except for the oxygens in the central layer and the Ti atom in the third layer. The largest charge changes are for the surface Ca ion and the subsurface O ion. The largest overall change in a layer charge ( $-0.234e$ ) appears in the subsurface layer as well.

For the O-terminated surface, the negative charge on the surface oxygen is very strongly decreased. Correspondingly, the second layer becomes substantially more negative (overall change  $-0.177e$ ) with the change coming mostly on the Ti atom. The total charge density on the third layer is almost unchanged. Negative changes in charge are observed on all central layer atoms leading to a total charge change of  $-0.055e$  in that layer.

The interatomic bond populations for the three terminations of the (011) surface are given in Table IX. The major effect observed here is a strong increase in the Ti-O chemical bonding near the TiO- and O-terminated surface as compared to bulk ( $0.084e$ ) or to what was found on the  $\text{TiO}_2$ -terminated (001) surface ( $0.114e$ ). For the O-terminated surface, the O(I)-Ti(II) bond population is about twice as large as in the bulk and about half again as large as at the  $\text{TiO}_2$ -terminated (001) surface. For the TiO-terminated (011) surface, the Ti-O bond populations are larger in the direction perpendicular to the surface ( $0.186e$ ) than in the plane ( $0.128e$ ).

#### IV. CONCLUSIONS

According to the results of our *ab initio* hybrid B3PW calculations, all of the upper-layer atoms for the  $\text{TiO}_2$ - and CaO-terminated  $\text{CaTiO}_3$  (001) surfaces relax inward, while outward relaxations of all atoms in the second layer are found at both kinds of (001) terminations. These results are typical for other technologically important  $\text{ABO}_3$  perovskites such as  $\text{BaTiO}_3$ ,  $\text{PbTiO}_3$ , and  $\text{BaZrO}_3$ .<sup>41,42,61,62</sup> However, they contrast with the only previous *ab initio* study of  $\text{CaTiO}_3$  (001) surfaces by Wang *et al.*,<sup>5</sup> where the authors found that the first-layer O atoms relax outward on the CaO-terminated (001) surface. For the  $\text{TiO}_2$ -terminated (001) surface, our largest relaxation is on the second-layer atoms, not on the first-layer ones, this time in agreement with Wang *et al.*<sup>5</sup> The stronger relaxation of the second-layer atoms compared to the first-layer ones was found by us earlier, also for  $\text{TiO}_2$ -terminated  $\text{PbTiO}_3$  and  $\text{SrTiO}_3$  (001) surfaces.<sup>7,41</sup> Our calculations of the CaO-terminated (001) surface show a very strong inward relaxation of 8.31% for the top-layer Ca atoms, in very good quantitative agreement with the inward



TABLE IX. The A-B bond populations  $P$  (in  $e$ ) and the relevant interatomic distances  $R$  (in Å) for three different (011) terminations of the  $\text{CaTiO}_3$  surface. Symbols I-IV denote the number of each plane enumerated from the surface. The nearest-neighbor Ti-O distance in the unrelaxed bulk is 1.926 Å.

Atom A	Atom B	$P$	$R$
TiO-terminated surface			
Ti(I)	O(I)	0.128	1.979
	O(II)	0.186	1.752
O(II)	Ti(III)	0.110	1.935
	Ca(III)	0.018	2.769
	O(III)	-0.024	2.790
Ti(III)	Ca(III)	0.000	3.336
	O(III)	0.100	1.929
	O(IV)	0.076	1.904
Ca(III)	O(III)	0.008	2.723
	O(IV)	0.004	2.672
O(III)	O(IV)	-0.032	2.653
Ca-terminated surface			
Ca(I)	O(II)	0.006	2.458
O(II)	Ca(III)	0.012	2.768
	Ti(III)	0.072	1.973
	O(III)	-0.036	2.784
Ca(III)	O(III)	0.002	2.723
	O(IV)	0.006	2.705
Ti(III)	O(III)	0.060	1.926
	Ca(III)	0.000	3.335
	O(IV)	0.084	1.915
O(III)	O(IV)	-0.064	2.691
O-terminated surface			
O(I)	Ca(II)	0.028	2.613
	Ti(II)	0.162	1.699
	O(II)	-0.016	2.788
Ca(II)	O(II)	-0.006	2.412
	Ti(II)	0.002	3.198
Ti(II)	O(II)	0.086	1.992
	O(III)	0.100	1.764
O(II)	O(III)	0.010	2.925
Ca(II)	O(III)	0.006	2.737
O(III)	O(IV)	-0.038	2.750
	Ti(IV)	0.062	1.963
	Ca(IV)	0.004	2.677

relaxation of 8.80% found by Wang *et al.*<sup>5</sup> This inward relaxation of the surface Ca atoms on the CaO-terminated (001) surface is much stronger than was obtained for the AO-terminated (001) surfaces of other  $\text{ABO}_3$  perovskites ( $A=\text{Sr, Ba, Pb, and Zr}$ ).<sup>7,41,42,61,62</sup>

Our calculated surface rumpling of 7.89% for the CaO-terminated (001) surface is almost five times larger than that of the corresponding  $\text{TiO}_2$ -terminated surface and is compa-

rable with the surface rumpling of 9.54% obtained for the CaO-terminated surface by Wang *et al.*<sup>5</sup> This rumpling is larger than the rumplings obtained in previous *ab initio* calculations for the AO-terminated (001) surfaces of  $\text{SrTiO}_3$ ,  $\text{BaTiO}_3$ ,  $\text{BaZrO}_3$ , and  $\text{PbTiO}_3$ .<sup>7,20,21,41,42,61,62</sup>

Our calculations predict a compression of the interlayer distance between first and second planes and an expansion between second and third planes for the (001) surfaces. Our value for  $\Delta d_{12}$  of -9.43% on the CaO-terminated (001) surface is in reasonable agreement with the result of -11.43% obtained by Wang *et al.*<sup>5</sup> and is larger than the corresponding value for  $\text{SrTiO}_3$ ,  $\text{BaTiO}_3$ ,  $\text{BaZrO}_3$ , and  $\text{PbTiO}_3$  (001) surfaces.<sup>7,20,21,41,42,61,62</sup> As for experimental confirmation of these results, we are unfortunately unaware of experimental measurements of  $\Delta d_{12}$  and  $\Delta d_{23}$  for the  $\text{CaTiO}_3$  (001) surfaces. Moreover, for the case of the SrO-terminated  $\text{SrTiO}_3$  (001) surface, existing LEED (Ref. 24) and RHEED (Ref. 25) experiments actually contradict each other regarding the sign of  $\Delta d_{12}$ . In view of the absence of clear experimental determinations of these parameters, therefore, the first-principles calculations are particularly important tool for understanding the surface properties.

Turning now to the  $\text{CaTiO}_3$  (011) surfaces, we found that the inward relaxation of the upper-layer metal atom on the TiO-terminated (011) surface (Ti displacement of 7.14%) is smaller than on the CaO-terminated (001) surface (Ca displacement of 8.31%), in contrast to what was found for the  $\text{SrTiO}_3$ ,  $\text{BaTiO}_3$ ,  $\text{PbTiO}_3$ , and  $\text{BaZrO}_3$  surfaces.<sup>7,20,21,41,42,61,62</sup> However, the inward relaxation by 16.05% of the upper-layer Ca atom on the Ca-terminated (011) surface is about twice as large as the inward relaxations of surface atoms obtained on the CaO-terminated (001) surface. Our calculated atomic displacements in the third plane from the surface for the Ca, TiO, and O-terminated (011) surfaces are still substantial. Our calculated surface rumpling  $s$  for the TiO-terminated (011) surface is approximately 1.5 times larger than that of the CaO-terminated (001) surface and many times larger than that of the  $\text{TiO}_2$ -terminated (001) surface. Also, our *ab initio* calculations predict a compression of the interlayer distance  $\Delta d_{12}$  and an expansion of  $\Delta d_{23}$  for the TiO- and O-terminated (011) surfaces. This behavior seems to be obeyed by all previous calculations of relaxations at (001)  $\text{ABO}_3$  perovskite surfaces;<sup>7,20,21,41,61,62</sup> we can conclude that this effect may be a general rule requiring further experimental studies and confirmation.

A comparison of our *ab initio* B3PW calculations on the TiO-terminated  $\text{CaTiO}_3$  (011) surface with the previous *ab initio* calculation performed by Zhang *et al.*<sup>6</sup> shows that the atomic displacement directions almost always coincide; the only exception being the small third-layer Ti-atom inward relaxation of -0.78% in our calculation compared with an outward one of 0.28% in theirs. The displacement magnitudes are generally comparable in the two studies leading to an excellent agreement for the TiO-terminated (011) surface rumplings (11.81% in our calculations vs 12.10% in theirs). For the Ca-terminated (011) surface, our inward relaxation magnitude of 16.05% for the upper-layer Ca atom—the largest of all atoms on all of the studied (011) terminations—is in excellent agreement with the value of 15.37% obtained in Ref. 6. This largest displacement of the surface A atom on



the A-terminated (011) surface was also obtained for the SrTiO<sub>3</sub>, BaTiO<sub>3</sub>, PbTiO<sub>3</sub>, and BaZrO<sub>3</sub> cases.<sup>7,20,21,41,42,61,62</sup> Just as they did for the TiO-terminated (011) surface, our relaxation directions for the Ca-terminated surface almost all coincide with those obtained previously:<sup>6</sup> the only exception being again the displacement direction of the third-layer Ti atom. We find that this atom moves slightly inward by 0.37%, whereas the previous work obtain an outward relaxation of 0.89%.<sup>6</sup>

For the O-terminated (011) surface, in most cases our calculated displacement directions are in qualitative agreement with the results of Ref. 6. In some cases, as for example for the second layer Ti and O atom displacements in the direction along the surface, our calculated displacement magnitudes for Ti (4.70%) and for O (8.05%) are in an excellent agreement with the corresponding results (4.53% and 8.06% respectively) of Zhang *et al.*<sup>6</sup> However, in many cases, our calculated displacement magnitude is smaller than that calculated in Ref. 6. Most disturbingly, in three cases there are also some qualitative differences between our results and those of Zhang *et al.*<sup>6</sup> Specifically, the second-layer Ca and Ti atoms move substantially inward in our calculations, but outward in Ref. 6, and the third-layer O atoms move in opposite directions in the two calculations.

As for the surface energies, we find that both the CaO- and TiO<sub>2</sub>-terminated (001) surfaces are about equally favorable with surface energies of 0.94 and 1.13 eV/cell, respectively. These values are in excellent agreement with the corresponding values of 0.82 and 1.02 eV/cell, respectively, as computed by Zhang *et al.* in Ref. 6. In contrast, we see very large differences in surface energies on the (011) surfaces. Our lowest-energy (011) surface is the O-terminated one at 1.86 eV/cell, with the Ca-terminated surface just behind at 1.91 eV/cell, and the TiO-terminated surface is very unfavorable at 3.13 eV/cell. These are all much larger by about a factor of 2 or more than for the (001) surfaces. This is the same ordering of (011) surface energies as was obtained by Zhang *et al.*, but these authors obtained quite different values of 0.84, 1.67, and 2.18 eV/cell for the O-, Ca-, and TiO-terminated (011) surfaces, respectively.<sup>6</sup> The values for the Ca- and TiO-terminated surface energies are only modestly smaller than ours; but the value for the O-terminated (011) surface energy presents a clear disagreement with the present work, being more than twice as small as ours. In fact, according to their work, the O-terminated (011) surface is even lower in energy than the TiO<sub>2</sub>-terminated (001) surface and about equal to that of the CaO-terminated (001) surface. In this respect, their result contrasts not only with our result for CaTiO<sub>3</sub>, but with all previous *ab initio* and shell-model calculations dealing with SrTiO<sub>3</sub>, BaTiO<sub>3</sub>, PbTiO<sub>3</sub>, and BaZrO<sub>3</sub> (001) and (011) surface energies,<sup>7,12,21,23,28,41,42</sup> where the (001) surface energies are always smaller than the (011) surface energies.

In order to test whether the discrepancy might result from the use of different exchange-correlation functionals (the hybrid B3PW functional used in our work vs the Perdew-Burke-Erzerhof generalized gradient approximation (PBE-GGA) functional<sup>64</sup> used by Zhang *et al.*), we have carried out test calculations of the (unrelaxed) cleavage energies of the three (011) surfaces using the PBE-GGA exchange-correlation functional, but implemented in the CRYSTAL-2003 code package, obtaining values of 4.47 and 3.17 eV/cell for the TiO/Ca and O terminations respectively. These values are only 3%–4% smaller than the hybrid B3PW values reported in Table VII, but still 15%–25% larger than the cleavage energies reported by Zhang *et al.*, indicating that the choice of exchange-correlation functional is not playing an important role. This suggests that the discrepancy must originate from the use of different computational codes (CRYSTAL-2003 in our case vs CASTEP in theirs) or from some technical choices such as cutoffs, pseudopotentials, or *k*-point sampling. One strange aspect, however, is that the pattern of relaxation energies looks quite different in the two calculations; while we obtain –1.48, –2.70, and –1.44 eV/cell for the TiO, Ca, and O-terminated (011) surfaces, they obtain –1.32, –1.83, and –1.93 eV/cell, respectively. The large relaxation energy of the O-terminated surface plays a dominant role in stabilizing that surface in their calculation. Therefore, as a further check, we also did a test PBE-GGA calculation of the energy of an O-terminated (011) slab in which the surface atoms were placed by hand at the coordinates reported for this surface in Ref. 6 and found that the energy was even higher than that of the unrelaxed structure. We thus remain skeptical of some of the results reported in Ref. 6.

Our *ab initio* calculations indicate a considerable increase in the Ti-O bond covalency near the TiO- and O-terminated (011) surfaces as well as the TiO<sub>2</sub>-terminated (001) surface. The Ti-O bond covalency at the TiO-terminated (011) surface (0.128*e*) is much larger than that for the TiO<sub>2</sub>-terminated (001) surface (0.114*e*) or in bulk CaTiO<sub>3</sub> (0.084*e*). The Ti-O bond populations on the TiO-terminated (011) surface are much larger in the direction perpendicular to the surface than in the plane (0.186 vs 0.128*e*). Our calculated increase in the Ti-O bond covalency near the (011) surface is in agreement with the resonant photoemission experiments.<sup>65</sup> This should have an impact on the electronic structure of surface defects (e.g., *F* centers),<sup>66</sup> as well as on the adsorption and surface diffusion of atoms and small molecules relevant for catalysis.

#### ACKNOWLEDGMENTS

The present work was supported by Deutsche Forschungsgemeinschaft (DFG) and by ONR with Grant No. N00014-05-1-0054.

- <sup>1</sup>J. F. Scott, *Ferroelectric Memories* (Springer, Berlin, 2000).
- <sup>2</sup>M. Dawber, K. M. Rabe, and J. F. Scott, *Rev. Mod. Phys.* **77**, 1083 (2005).
- <sup>3</sup>R. E. Cohen, *Nature (London)* **358**, 136 (1992).
- <sup>4</sup>A. E. Ring, S. E. Kesson, K. D. Reeve, D. M. Levins, and E. J. Ramm, in *Radioactive Waste Forms for the Future*, edited by W. Lutze and R. C. Ewings (North-Holland, Amsterdam, 1987).
- <sup>5</sup>Y. X. Wang, M. Arai, T. Sasaki, and C. L. Wang, *Phys. Rev. B* **73**, 035411 (2006).
- <sup>6</sup>J. M. Zhang, J. Cui, K. W. Xu, V. Ji, and Z. Y. Man, *Phys. Rev. B* **76**, 115426 (2007).
- <sup>7</sup>R. I. Eglitis and D. Vanderbilt, *Phys. Rev. B* **77**, 195408 (2008).
- <sup>8</sup>S. Kimura, J. Yamauchi, M. Tsukada, and S. Watanabe, *Phys. Rev. B* **51**, 11049 (1995).
- <sup>9</sup>Z. Q. Li, J. L. Zhu, C. Q. Wu, Z. Tang, and Y. Kawazoe, *Phys. Rev. B* **58**, 8075 (1998).
- <sup>10</sup>R. Herger, P. R. Willmott, O. Bunk, C. M. Schlepütz, B. D. Patterson, and B. Delley, *Phys. Rev. Lett.* **98**, 076102 (2007).
- <sup>11</sup>N. Erdman, K. Poepfelmeier, M. Asta, O. Warschkow, D. E. Ellis, and L. Marks, *Nature (London)* **419**, 55 (2002).
- <sup>12</sup>E. Heifets, R. I. Eglitis, E. A. Kotomin, J. Maier, and G. Borstel, *Phys. Rev. B* **64**, 235417 (2001).
- <sup>13</sup>E. Heifets, R. I. Eglitis, E. A. Kotomin, J. Maier, and G. Borstel, *Surf. Sci.* **513**, 211 (2002).
- <sup>14</sup>K. Johnston, M. R. Castell, A. T. Paxton, and M. W. Finnis, *Phys. Rev. B* **70**, 085415 (2004).
- <sup>15</sup>R. I. Eglitis, S. Piskunov, E. Heifets, E. A. Kotomin, and G. Borstel, *Ceram. Int.* **30**, 1989 (2004).
- <sup>16</sup>S. Piskunov, E. A. Kotomin, E. Heifets, J. Maier, R. I. Eglitis, and G. Borstel, *Surf. Sci.* **575**, 75 (2005).
- <sup>17</sup>R. Herger, P. R. Willmott, O. Bunk, C. M. Schlepütz, B. D. Patterson, B. Delley, V. L. Shneerson, P. F. Lyman, and D. K. Saldin, *Phys. Rev. B* **76**, 195435 (2007).
- <sup>18</sup>C. H. Lanier, A. van de Walle, N. Erdman, E. Landree, O. Warschkow, A. Kazimirov, K. R. Poepfelmeier, J. Zegenhagen, M. Asta, and L. D. Marks, *Phys. Rev. B* **76**, 045421 (2007).
- <sup>19</sup>Y. L. Li, S. Choudhury, J. H. Haeni, M. D. Biegalski, A. Vasudevarao, A. Sharan, H. Z. Ma, J. Levy, V. Gopalan, S. Trolier-McKinstry, D. G. Schlom, Q. X. Jia, and L. Q. Chen, *Phys. Rev. B* **73**, 184112 (2006).
- <sup>20</sup>C. Cheng, K. Kunc, and M. H. Lee, *Phys. Rev. B* **62**, 10409 (2000).
- <sup>21</sup>J. Padilla and D. Vanderbilt, *Surf. Sci.* **418**, 64 (1998).
- <sup>22</sup>V. Ravikumar, D. Wolf, and V. P. Dravid, *Phys. Rev. Lett.* **74**, 960 (1995).
- <sup>23</sup>E. Heifets, E. A. Kotomin, and J. Maier, *Surf. Sci.* **462**, 19 (2000).
- <sup>24</sup>N. Bickel, G. Schmidt, K. Heinz, and K. Müller, *Phys. Rev. Lett.* **62**, 2009 (1989).
- <sup>25</sup>T. Hikita, T. Hanada, M. Kudo, and M. Kawai, *Surf. Sci.* **287-288**, 377 (1993).
- <sup>26</sup>M. Kudo, T. Hikita, T. Hanada, R. Sekine, and M. Kawai, *Surf. Interface Anal.* **22**, 412 (1994).
- <sup>27</sup>Y. Kido, T. Nishimura, Y. Hoshido, and H. Mamba, *Nucl. Instrum. Methods Phys. Res. B* **161-163**, 371 (2000).
- <sup>28</sup>G. Charlton, S. Brennan, C. A. Murny, R. McGrath, D. Norman, T. S. Turner, and G. Thornton, *Surf. Sci.* **457**, L376 (2000); E. Heifets, W. A. Goddard, E. A. Kotomin, R. I. Eglitis, and G. Borstel, *Phys. Rev. B* **69**, 035408 (2004).
- <sup>29</sup>H. Bando, Y. Aiura, Y. Haruyama, T. Shimizu, and Y. Nishihara, *J. Vac. Sci. Technol. B* **13**, 1150 (1995).
- <sup>30</sup>K. Szot and W. Speier, *Phys. Rev. B* **60**, 5909 (1999).
- <sup>31</sup>J. Brunen and J. Zegenhagen, *Surf. Sci.* **389**, 349 (1997).
- <sup>32</sup>Q. D. Jiang and J. Zegenhagen, *Surf. Sci.* **425**, 343 (1999).
- <sup>33</sup>J. Zegenhagen, T. Haage, and Q. D. Jiang, *Appl. Phys. A: Mater. Sci. Process.* **67**, 711 (1998).
- <sup>34</sup>R. Souda, *Phys. Rev. B* **60**, 6068 (1999).
- <sup>35</sup>Y. Adachi, S. Kohiki, K. Wagatsuma, and M. Oku, *J. Appl. Phys.* **84**, 2123 (1998).
- <sup>36</sup>F. Bottin, F. Finocchi, and C. Noguera, *Phys. Rev. B* **68**, 035418 (2003).
- <sup>37</sup>A. Asthagiri and D. Sholl, *Surf. Sci.* **581**, 66 (2005).
- <sup>38</sup>A. D. Becke, *J. Chem. Phys.* **98**, 5648 (1993).
- <sup>39</sup>J. P. Perdew and W. Yue, *Phys. Rev. B* **33**, 8800 (1986); **40**, 3399(E) (1989); J. P. Perdew and Y. Wang, *Phys. Rev. B* **45**, 13244 (1992).
- <sup>40</sup>E. Heifets, J. Ho, and B. Merinov, *Phys. Rev. B* **75**, 155431 (2007).
- <sup>41</sup>R. I. Eglitis and D. Vanderbilt, *Phys. Rev. B* **76**, 155439 (2007).
- <sup>42</sup>R. I. Eglitis, *J. Phys.: Condens. Matter* **19**, 356004 (2007).
- <sup>43</sup>V. R. Saunders, R. Dovesi, C. Roetti, M. Causa, N. M. Harrison, R. Orlando, and C. M. Zicovich-Wilson, *CRYSTAL-2003 User Manual* (University of Torino, Torino, Italy, 2003).
- <sup>44</sup>S. Piskunov, E. Heifets, R. I. Eglitis, and G. Borstel, *Comput. Mater. Sci.* **29**, 165 (2004).
- <sup>45</sup>H. Shi, R. I. Eglitis, and G. Borstel, *Phys. Rev. B* **72**, 045109 (2005).
- <sup>46</sup>P. J. Hay and W. R. Wadt, *J. Chem. Phys.* **82**, 270 (1985); **82**, 284 (1985); **82**, 299 (1985).
- <sup>47</sup>H. J. Monkhorst and J. D. Pack, *Phys. Rev. B* **13**, 5188 (1976).
- <sup>48</sup>C. Noguera, *J. Phys.: Condens. Matter* **12**, R367 (2000).
- <sup>49</sup>P. W. Tasker, *J. Phys. C* **12**, 4977 (1979).
- <sup>50</sup>A. Pojani, F. Finocchi, and C. Noguera, *Surf. Sci.* **442**, 179 (1999).
- <sup>51</sup>A. Granicher and O. Jakits, *Nuovo Cimento, Suppl.* **11**, 480 (1954).
- <sup>52</sup>H. F. Kay and P. C. Bailey, *Acta Crystallogr.* **10**, 219 (1957).
- <sup>53</sup>X. Liu and R. C. Liebermann, *Phys. Chem. Miner.* **20**, 171 (1993).
- <sup>54</sup>B. J. Kennedy, C. J. Howard, and B. C. Chakoumakos, *J. Phys.: Condens. Matter* **11**, 1479 (1999).
- <sup>55</sup>A. M. Glazer, *Acta Crystallogr., Sect. B: Struct. Crystallogr. Cryst. Chem.* **28**, 3384 (1972).
- <sup>56</sup>D. Vanderbilt and W. Zhong, *Ferroelectrics* **206**, 181 (1998).
- <sup>57</sup>E. Cockayne and B. P. Burton, *Phys. Rev. B* **62**, 3735 (2000).
- <sup>58</sup>*Ferroelectrics and Related Substances*, Landolt-Bornstein, New Series, Group III, Vol. 3, edited by K. H. Hellwege and A. M. Hellwege (Springer, Berlin, 1969).
- <sup>59</sup>C. R. A. Catlow and A. M. Stoneham, *J. Phys. C* **16**, 4321 (1983).
- <sup>60</sup>R. C. Bochicchio and H. F. Reale, *J. Phys. B* **26**, 4871 (1993).
- <sup>61</sup>J. Padilla and D. Vanderbilt, *Phys. Rev. B* **56**, 1625 (1997).
- <sup>62</sup>B. Meyer, J. Padilla, and D. Vanderbilt, *Faraday Discuss.* **114**, 395 (1999).

<sup>63</sup>K. Rapcewicz, B. Chen, B. Yakobson, and J. Bernholc, Phys. Rev. B **57**, 7281 (1998).

<sup>64</sup>J. P. Perdew, K. Burke, and M. Ernzerhof, Phys. Rev. Lett. **77**, 3865 (1996).

<sup>65</sup>R. Courths, B. Cord, and H. Saalfeld, Solid State Commun. **70**, 1047 (1989).

<sup>66</sup>R. I. Eglitis, N. E. Christensen, E. A. Kotomin, A. V. Postnikov, and G. Borstel, Phys. Rev. B **56**, 8599 (1997).